Turkish Journal of Chemistry

http://journals.tubitak.gov.tr/chem/

Research Article

Turk J Chem
(2019) 43: 1040 – 1051

doi:10.3906/kim-1903-6

Targeting human telomeric DNA with azacyanines

Ayça KÜÇÜKAKDAĞ DOĞU, Özgül PERSİL ÇETİNKOL*
Department of Chemistry, Faculty of Arts and Sciences, Middle East Technical University, Ankara, Turkey

Received: 01.03.2019 • **Accepted/Published Online:** 29.03.2019 • **Final Version:** 06.08.2019

Abstract: Small molecules targeting telomeric DNA or its interactions with telomerase have been an active area of cancer research. In the present study, we investigated the interactions of six benzimidazole compounds, called azacyanines, differing from each other in alkyl chain length and branching in the benzimidazole ring (azamethyl, azaethyl, azapropyl, azaisopropyl, azabutyl, and azaisobutyl) with human telomeric DNA (tel24) in 1:1 and 1:6 ratio (tel24:azacyanine) using UV-Vis, circular dichroism (CD), and fluorescence spectroscopy. All the compounds were binding to tel24 as indicated by the formation of the weak induced CD band between 320 nm and 360 nm. A substantial red shift and hypochromic effect were observed in the UV-Vis spectrum of azamethyl or azabutyl upon binding to tel24. No red shift or hypochromic effect was observed in the spectrum of azaisopropyl. The denaturation temperature (T_m) of tel24 increased the most, from 65 °C to 78 °C, in the presence of azabutyl in 1:6 ratio. Azaisopropyl stabilized tel24 the least under the same conditions. The highest ($7.84 \times 10^5 \pm 3.44 \times 10^4$ M^{-1}) and the lowest ($2.04 \times 10^5 \pm 5.38 \times 10^4$ M^{-1}) association constants were obtained for azabutyl and azaisopropyl, respectively, by fluorescence spectroscopy. Overall, the benzimidazole scaffold, the one-pot synthesis, and the stabilization ability of azacyanines to tel24 make them plausible drug candidate molecules in targeting G-quadruplexes.

Key words: G-quadruplex, human telomeric DNA, azacyanine, small molecule binding, intercalation

1. Introduction

Genome-wide analyses have revealed that guanine-rich sequences are present in the human genome, particularly at the end of the chromosomes and telomeres, and in promoter regions such as those seen in the c-myc gene [1–6]. Human telomeres, essential for the integrity of the chromosomes, are composed of thousands of double-stranded tandem repeats of d(TTAGGG) and a single stranded G rich 3′ overhang of about 100–200 nucleotides [1–6]. Targeting telomeres via small molecules has been one of the active areas of research in cancer therapy in the last two decades. Due to the end-replication problem, telomeres in our somatic cells are shortened in each cell division where a critical telomere length signals the cell cycle arrest. However, in 80%–85% of cancer cells, the end-replication problem is found to be solved with the help of an active telomerase enzyme. Telomerase that is kept inactive in somatic cells has been found to maintain the telomere length in cancer cells and consequently delay cell cycle arrest [7–13].

One of the approaches commonly exploited in drug design for stimulating cell cycle arrest in cancer cells is to alter or abolish telomere–telomerase interactions by stabilizing G-quadruplex structures using small molecules. G-quadruplex structures are formed within the guanine-rich sequences via stacking of two or more G-quartets, where G-quartets are formed from four guanine bases. Several small molecules stabilizing G-

*Correspondence: opersil@metu.edu.tr

quadruplex structures have been discovered and even included in clinical trials in the last decade. CX-5461, telomestatin, Braco-19, RHPS4, and 307A are such small molecules [9,14–18]. Most of these ligands are positively charged extended aromatic systems that interact with the negatively charged DNA backbone and can stack with G-quartets at the same time. In our previous efforts to identify such G-quadruplex stabilizing small molecules, we realized that the benzimidazole and benzothiazole derivative azacyanines were stabilizing human telomeric sequences tel24 and tel26 [11–13,19]. More importantly, azacyanines were selective against quadruplex structures, which is a desirable attribute in drug design. We revealed that azacyanine 3 (named azamethyl here) was binding to a quadruplex, forming a tel24 ([d(TTGGG(TTAGGG)$_3$A)]) sequence almost 200 times more selective than the duplex forming dd1 sequence ([d(GCGCATATATGCGC)]). NMR studies indicated that azamethyl was binding in between the top G-quartet and A-T base pair found in the loop region of tel24 with a dissociation constant in the low micromolar region in 1:1 ratio [19].

Benzimidazole is considered an important scaffold in the design and synthesis of pharmacophores and thus is commonly exploited [20–23]. Several studies investigating the effect of the benzimidazole scaffold on telomeric DNA and oncogene promoters such as KRAS and VEGFR that are known to fold into quadruplex structures were recently reported [24–30]. In addition, several reports investigating the effect of such small molecules on different cancer lines and promoting G-quadruplexes as plausible targets in cancer therapy were also published [31–36]. Based on all these reported studies and our knowledge on azamethyl, we were inspired to explore a series of azacyanine compounds as potential G-quadruplex stabilizing compounds with the hope of finding a better candidate than azamethyl and understanding the effect of molecular structure on molecular recognition. In the present study, we evaluated the interactions of benzimidazole derivatives, differing from azamethyl in alkyl chain length and branching, with tel24 using UV-Vis, fluorescence, and CD spectroscopy and tried to reveal the effect of molecular structure on G-quadruplex binding [37]. To the best of our knowledge, this is a unique study revealing the effect of chain length and branching on G-quadruplex recognition.

2. Results and discussion

2.1. Determination of binding using UV-Vis and CD spectroscopy

The interactions of azacyanines with tel24 were first investigated using UV-Vis and circular dichroism (CD) spectroscopy in order to quickly survey and confirm the presence of interactions between the azacyanines and tel24. Such a survey also reveals changes in the secondary structure of tel24 upon azacyanine binding and the effect of azacyanine structure on tel24 binding [25,28–37]. Our previous structural studies using NMR have shown that one azamethyl was binding to one tel24 G-quadruplex structure between the top quartet and the A-T base pairing in the loop region. A second binding site was observed at the bottom of the quartet. However, binding to that site was very weak as it was not observed in fluorescence or surface plasmon resonance (SPR) spectroscopy. Only one binding site was determined via fluorescence titrations and SPR measurements [19]. Therefore, in our current study we first investigated 1:1 tel24:azacyanine complexes.

The CD spectra of tel24:azacyanine 1:1 complexes revealed that all the azacyanines were interacting with tel24, as a very weak CD band, induced by tel24, between 320 nm and 360 nm is observed in the presence of tel24 in all azacyanines' spectra (Figure 1). DNA bases do not absorb light above 300 nm, and therefore as expected tel24 by itself did not give rise to any CD signal above 300 nm (Figure 1, dotted black line). On the other hand, azacyanines did not give rise to the formation of any CD signal by themselves since they are achiral molecules (Figure 1, dotted red line). However, the binding of an azacyanine to the chiral environment of tel24

gave rise to the formation of the CD band between 320 nm and 360 nm. Therefore, this band, also referred as the "induced CD band", confirms the interactions between tel24 and azacyanines. The shapes of the induced CD bands were similar in all azacyanines with two absorbance maximums at around 330 nm and 342 nm. The intensity of the induced CD band showed slight variation between azacyanines.

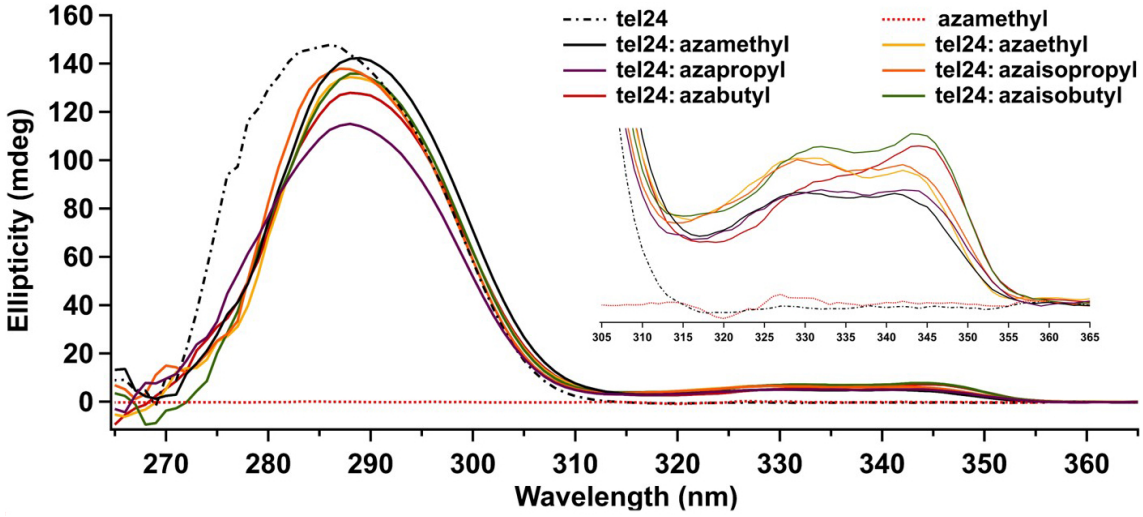

Figure 1. CD spectra of tel24 (25 μM in strand) in the absence and presence of 25 μM azacyanines (1:1) at 5 °C. Inset shows the induced CD band region; all azacyanines gave no CD signal in the absence of DNA. Only azamethyl was shown here for simplicity.

Next, thermal denaturation studies were performed in order to reveal the effect of azacyanines on tel24's stability. Thermal denaturation studies of tel24 in the presence of azacyanines revealed that all the azacyanines except azaisopropyl were stabilizing the structure slightly in 1:1 tel24:azacyanine (2.5 μM tel24 in strand:2.5 μM azacyanine) complexes (Table 1).

The thermal denaturation temperature (T_m) of tel24 by itself was 65 °C. Tel24 was stabilized by azamethyl and azabutyl the most, where T_m was increased to 68 °C. We wondered whether increasing the azacyanine concentration would stabilize the tel24 structure further and lead to a discrimination between the azacyanine molecules in terms of their tel24 stabilization ability. Therefore, we investigated the thermal denaturation behavior of tel24 under increased concentrations of small molecules according to the nearest neighbor exclusion principle. The samples studied were 25 μM in strand (60 μM in base) tel24 and 150 μM small molecule (denoted as 1:6 ratio). UV-Vis thermal denaturation studies revealed that the stability of tel24 was increasing in the presence of increased azacyanine concentrations. The azaisopropyl had the least effect again on stability, increasing the T_m of tel24 only by 3 °C. On the other hand, azabutyl had the most dramatic effect, followed by azaisobutyl. Azabutyl increased the T_m of tel24 to 78 °C and azaisobutyl increased T_m to 77 °C compared to 75 °C by azamethyl (Table 1).

In our previous efforts, we observed a hypochromic effect and a red shift in azamethyl's UV-Vis bands between 305 nm and 360 nm. These changes in the UV-Vis spectra are generally associated with intercalation as the mode of binding and we verified the mode of binding as intercalation via 2D NMR studies in azamethyl binding to tel24 [19,38–40]. Here, we also compared the spectrum of 1:1 tel24:azacyanine complexes at 20 °C and 95 °C as representatives of the bound and the unbound state of the corresponding azacyanine, respectively. As mentioned above, by itself tel24 has a T_m of 65 °C and this T_m value was increased to higher values

Table 1. UV-Vis thermal denaturation temperatures obtained from the first heating scans of tel24 in the absence and presence of azacyanines.

Compounds	T_m (°C), tel24:azacyanine (1:1)	T_m (°C), tel24:azacyanine (1:6)
Tel24	65	65
azamethyl	68	75
azaethyl	66	72
azapropyl	66	73
azaisopropyl	65	68
azabutyl	68	78
azaisobutyl	66	77

due to binding of azacyanines. Consequently, at 20 °C azacyanines are expected to be found bound to the folded tel24 G-quadruplex structure. On the other hand, at 95 °C, a temperature higher than the T_m of tel24, the G-quadruplex is denatured and all the azacyanines are expected to dissociate from the G-quadruplex structure. When we compared the UV-Vis spectra of all the 1:1 tel24:azacyanine complexes at 20 °C and 95 °C as representatives of the bound and the unbound state of the corresponding azacyanine, respectively, a hypochromic effect similar to azamethyl's was observed only in azabutyl's and azaisobutyl's UV-Vis spectra (Figure 2). The hypochromic effect observed in azabutyl's was higher, which actually correlates with tighter binding. Furthermore, the red shift observed was the most obvious in azabutyl's spectrum. We did not observe any hypochromic effect in azaisopropyl's spectrum upon binding. Again, this correlates with the lowest increase in T_m of tel24 upon azaisopropyl's binding. When comparing the spectra of all the azacyanines, one thing that was noted was the similarity between the spectra of all azacyanines at 95 °C. They all had the same characteristic features. On the other hand, the UV-Vis spectrum of azamethyl at 20 °C was distinctly different from the other azacyanines' spectra.

When we compared the UV-Vis spectra of 1:6 tel24:azacyanine complexes, we observed a hypochromic effect and a very slight red shift only in the UV-Vis spectrum of tel24:azamethyl. We think the stacking of small molecules on the sides of the G-quadruplex dominates the intercalative mode of binding and causes the disappearance of the red shift at high azacyanine concentrations in 1:6 complexes (Figure 3).

We also investigated the 1:6 tel24:azacyanine complexes via CD spectroscopy (Figure 4). Compared to 1:1 samples, a weak induced CD band was also observed for 1:6 samples. However, the induced CD bands had only one maximum absorbance that is red shifted compared to 1:1 samples. The change in the shape of the CD bands also indicates the change in the binding mode of the azacyanines when present at relatively high concentrations compared to tel24. A second binding site was observed previously for the binding of azamethyl to tel24 via NMR studies where the concentration of tel24 and azamethyl were relatively high compared to the samples used in spectroscopic analysis [19,38–40]. We think in a similar way that the intercalative mode of binding might be dominated by a second or a third kind of binding mode such as the stacking of azacyanines on the bottom and/or the sides of the G-quadruplex structure when present at relatively high concentrations.

2.2. Determination of association constants using fluorescence spectroscopy

Finally, the association constants of azacyanines with tel24 were determined using fluorescence spectroscopy in order to reveal the effect of molecular structure on the binding strength. The fluorescence spectra were obtained

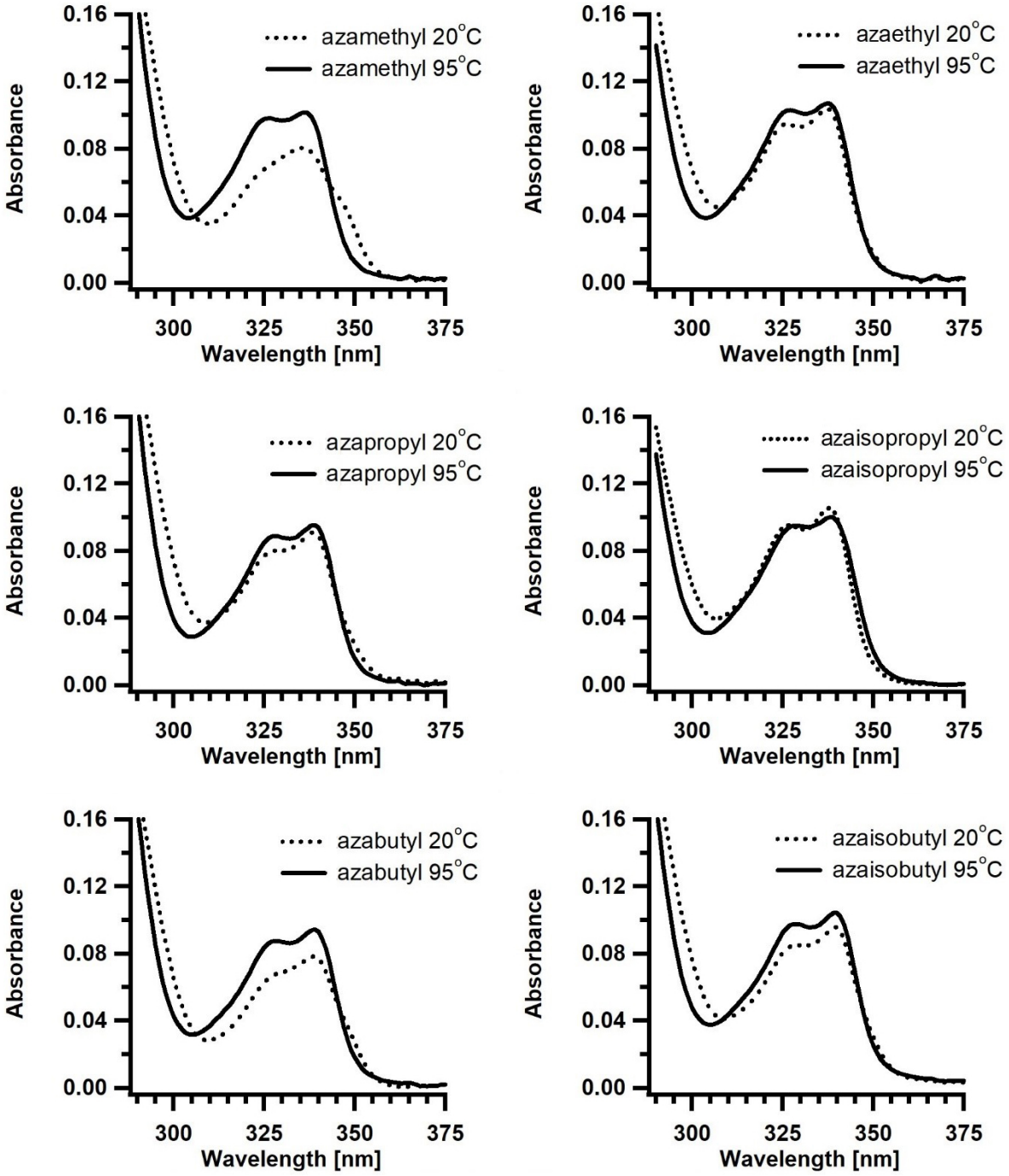

Figure 2. UV-Vis absorbance of 1:1 tel24 azacyanine (2.5 μM tel24 in strand:2.5 μM small molecule) complexes at 20 °C and 95 °C.

by tracing the decrease in the fluorescence intensity of azacyanines while titrating the 1 μM azacyanine solution with 50 μM in strand–1 μM tel24–azacyanine solution, until the fluorescence intensity remained constant. The binding constants were obtained by fitting the integrated fluorescence intensity data as a function of DNA concentration. The experimental details are given in the Materials and methods section [41,42]. We observed

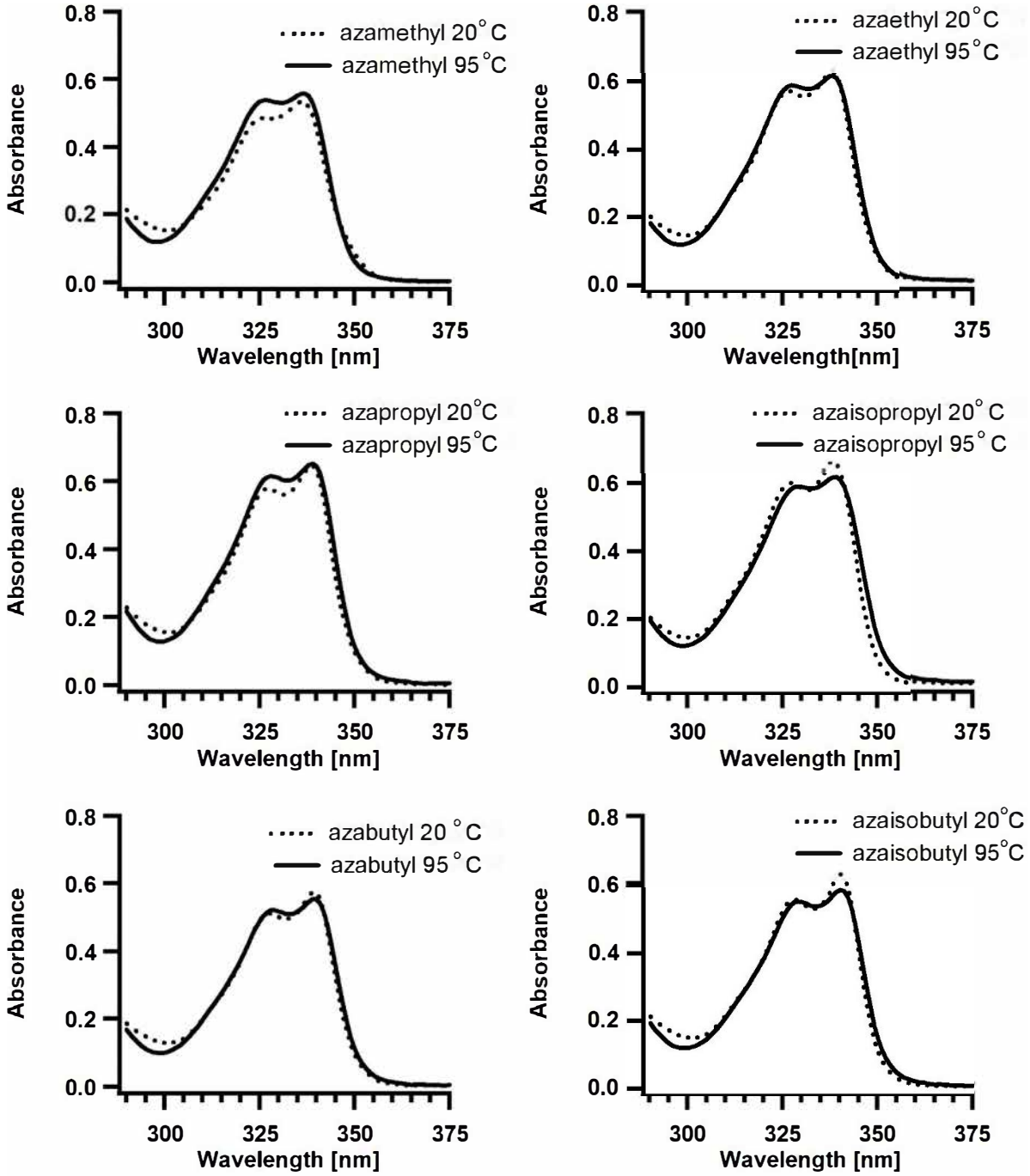

Figure 3. UV-Vis absorbance of 1:6 tel24–azacyanine (2.5 μM tel 24 in strand:15 μM small molecule) complexes at 20 °C and 95 °C.

one tight binding site in fluorescence titrations. Our fluorescence titrations confirmed the results of thermal denaturation experiments. Tel24:azabutyl had the highest association constant, $7.84 \times 10^5 \pm (3.44 \times 10^4)$ M^{-1} and tel24:azaisopropyl had the lowest association constant, $2.04 \times 10^5 \pm (5.38 \times 10^4)$ M^{1}. In agreement with thermal denaturation studies, tel24:azamethyl had the second highest association constant, $6.61 \times 10^5 \pm (3.74 \times 10^4)$ M^{-1} (Table 2).

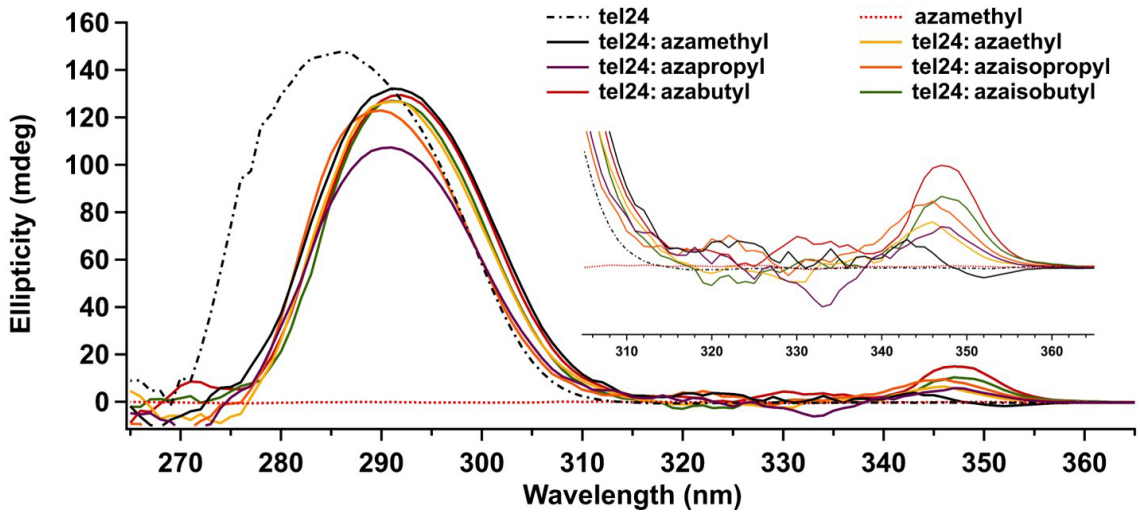

Figure 4. CD spectra of tel24 (25 μM in strand) in the absence and presence of 150 μM azacyanines (1:6) at 5 °C. Insert shows the induced band region; all azacyanines gave no CD signal in the absence of DNA. Only azamethyl was shown here for simplicity.

Table 2. Association constants determined by fluorescence spectroscopy for azacyanines with tel24.

Compounds	Association constant (M^{-1})
Azamethyl	$6.61 \times 10^5 \pm (3.74 \times 10^4)$
Azaethyl	$2.57 \times 10^5 \pm (5.40 \times 10^4)$
Azapropyl	$3.63 \times 10^5 \pm (4.06 \times 10^4)$
Azaisopropyl	$2.04 \times 10^5 \pm (5.38 \times 10^4)$
Azabutyl	$7.84 \times 10^5 \pm (3.44 \times 10^4)$
Azaisobutyl	$4.55 \times 10^5 \pm (1.23 \times 10^4)$

In conclusion, herein we investigated the interactions of azamethyl, azaethyl, azapropyl, azaisopropyl, azabutyl, and azaisobutyl with G-quadruplex forming human telomeric DNA, tel24. We found that all the azacyanines were interacting with tel24 and stabilizing the G-quadruplex structure as evident by CD, UV-Vis, and florescence spectroscopy. The stabilization degree was not directly related to the alkyl chain length or the branching on the benzimidazole ring. Azabutyl was stabilizing the tel24 structure the most, followed by azamethyl and azaisobutyl groups. Azaisopropyl was the least stabilizing molecule as evident both from the UV-Vis thermal denaturation experiments and fluorescence titrations. Previously, azamethyl was found to be intercalating between the top G-quartet and A-T base pairing in the loop region. We suspect that the short bulky isopropyl group might be preventing the slide of the azacyanine as an intercalator in between the base pairs. On the other hand, having a longer alkyl chain on the benzimidazole ring might also be interfering with intercalation since azaethyl and azapropyl were stabilizing the G-quadruplex structure less compared to azamethyl. However, once the length of the alkyl chain is long and flexible enough as in the case of azabutyl, the long chain can still be interfering with the intercalation but the increased hydrophobic interactions between the butyl chain and the quadruplex structure might be compensating for that. Our studies also demonstrated that while the degree of red shift and the hypochromic effect are an indication of tighter binding in the same class of small molecules binding to nucleic acids, the intensity of the induced CD band was not.

The benzimidazole scaffold, the one-pot synthesis, and the ease of purification of azacyanines make them plausible candidates in the development of new G-quadruplex binding small molecules. Here we found that azabutyl was binding to tel24 more tightly compared to azamethyl. Our efforts will continue with decorating the azabutyl chain and/or the benzimidazole ring with additional H-bonding donor and acceptor functional groups to increase binding affinity towards G-quadruplex structures.

3. Materials and methods

3.1. Materials

The oligonucleotide used in the experiments, tel24 ([d(TTGGG(TTAGGG)$_3$A)]), was purchased from Integrated DNA Technologies (Europe). Stock concentrations were calculated by using the extinction coefficients provided by the supplier. 2-Amino-1-methyl-benzimidazole, 1-ethyl-1H-benzimidazole-2-ylamine, 1-isopropyl-1H-benzimidazole-2-ylamine, 1-butyl-1H-benzimidazole-2-ylamine, and 1-isobutyl-1H-benzimidazole-2-ylamine were purchased from either Sigma Aldrich (Europe) or abcr (Germany). 1-Propyl-1H-benzimidazole-2-ylamine was purchased from Ark Pharm (USA). Diiodomethane was purchased from Sigma Aldrich (Europe) or TCI Chemicals (Europe). All the other solvents were purchased from Sigma Aldrich (Europe). All samples were prepared in 25 mM potassium phosphate buffer (pH 7.0) and 70 mM KCl, unless otherwise stated. Samples were annealed by heating to 95 °C for 5 min in a water bath and then cooling overnight to room temperature prior to each experiment (19, 25, 33).

3.2. Synthesis of benzimidazole derivatives

All benzimidazole derivatives were synthesized and characterized according to the previously reported methods (Figure 5) [19,31,43,44]. The stock concentrations were determined using the previously reported extinction coefficients of the compounds in DMSO using UV-Vis spectroscopy. The final DMSO concentration was less than 1% in our samples, containing small molecules, used in the fluorescence and UV-Vis thermal denaturation experiments (1:1 tel24:azacyanine samples). The final DMSO concentration was less than 5% in 1:6 tel24:azacyanine samples used in the UV-Vis thermal denaturation experiments and 1:1 tel24:azacyanine samples used in the CD. The final DMSO concentration was less than 10% in 1:6 tel24:azacyanine samples used in the CD.

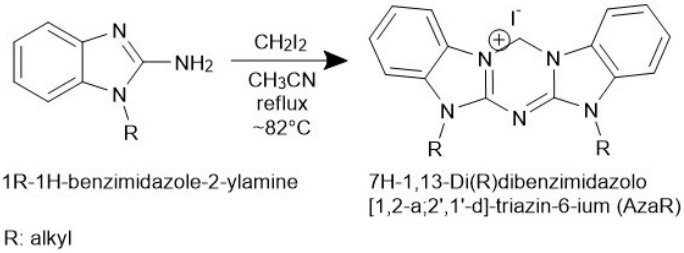

Figure 5. The synthesis of benzimidazole derivatives. R is the alkyl group: methyl, ethyl, propyl, isopropyl, butyl, or isobutyl.

3.3. UV-Vis thermal denaturation experiments

An Agilent HP 8454 UV-Vis diode array spectrophotometer equipped with an Agilent 89090A Peltier temperature control unit was used in the UV-Vis and thermal denaturation studies. The samples were heated from 20 °C to 95 °C with a 1 °C/min heating rate and the UV-Vis spectrum was collected at each 1 °C step

between 190 nm and 1100 nm. For the baseline correction 25 mM potassium phosphate buffer (pH 7.00) with 70 mM potassium chloride was used as blank.

3.4. Circular dichroism (CD) spectroscopy

CD spectra were acquired on a JASCO J-815 CD spectropolarimeter equipped with a Peltier temperature control unit. The CD spectra were collected from 240 nm to 400 nm at 5 °C at 200 nm/min scanning speed with 1 nm band width. Moreover, 25 mM potassium phosphate buffer (pH 7.00) with 70 mM potassium chloride was used as blank and all the CD spectra were baseline corrected.

3.5. Fluorescence titrations

Binding constants of all azacyanines with tel24 were determined using a Cary Eclipse fluorescence spectrophotometer as previously described [19,41,42]. Fluorescence titrations were performed by making incremental additions of 50 μM tel24 stock solution containing 1.0 μM azacyanine into the sample containing only 1.0 μM azacyanine. Excitation wavelength of 324 nm was used, and the emission spectra were collected from 325 to 675 nm. The excitation slit was set to 2.5 nm and the emission slit was set to 5.0 nm. Binding constants were obtained by fitting the integrated fluorescence intensity data between 335 nm and 600 nm as a function of DNA concentration using the least squares equations:

$$KC_b^2 - C_b(KS_0 + KD_0 + 1) + KS_0D_0 = 0$$

$$F = F_0(C_t - C_b) + F_bC_b,$$

where K is the association constant (in M^{-1}), C_b is the concentration of bound ligand, S_0 is the total binding site concentration, C_t is the total concentration of small molecule, D_0 is the total ligand concentration, F is observed fluorescence at each titration point, F_0 is fluorescence intensity of the free small molecule, and F_b is the fluorescence of the bound species [42]. Igor Pro software (Wavemetrics Inc, USA) was used in all of our data analysis. Data were obtained as an average of three replicates for each tel24:azacyanine titration.

Acknowledgments

This work was supported by grants from L'Oréal-UNESCO for Women in Science Turkey Scholarship and METU-BAP (BAP-08-11-2016-026). The synthesis of some of the azacyanines was also supported by TÜBİTAK (116Z219). We thank Prof Dr Ahmet Önal's group at METU for the fluorescence spectroscopy measurements. We would like to thank Aynur Özel and Serra Tütüncü for their help with the CD spectroscopy.

References

1. Phan AT, Mergny JL. Human telomeric DNA: G-quadruplex, I-motif and Watson-Crick double helix. Nucleic Acids Research 2002; 30 (21): 4618-4625. doi: 10.1093/nar/gkf597
2. Huppert JL, Balasubramanian S. Prevalence of quadruplexes in the human genome. Nucleic Acids Research 2005; 33 (9): 2908-2916. doi: 10.1093/nar/gki609
3. Chambers VS, Marsico G, Boutell JM, Di Antonio M, Smith GP et al. High-throughput sequencing of DNA G-quadruplex structures in the human genome. Nature Biotechnology 2015; 33 (8): 877-881. doi: 10.1038/nbt.3295
4. Burge S, Parkinson GN, Hazel P, Todd AK. Quadruplex DNA: sequence, topology and structure. Nucleic Acids Research 2006; 34 (19): 5402-5415. doi: 10.1093/nar/gkl655

5. Yang D, Hurley LH. Structure of the biologically relevant G-quadruplex in the c-MYC promoter. Nucleosides, Nucleotides and Nucleic Acids 2006; 25 (8): 951-968. doi: 10.1081/15257770600809913

6. Siddiqui-Jain A, Grand CL, Bearss DJ, Hurley LH. Direct evidence for a G-quadruplex in a promoter region and its targeting with a small molecule to repress c-*MYC* transcription. Proceedings of the National Academy of Sciences 2002; 99 (18): 11593-11598. doi: 10.1073/pnas.182256799

7. Greider CW. Telomerase activity, cell proliferation, and cancer. Proceedings of the National Academy of Sciences 1998; 95 (1): 90-92. doi: 10.10737pnas.95.1.90

8. Wright WE, Shay JW. Role of telomeres and telomerase in cancer. Seminars in Cancer Biology 2011; 21 (6): 349-353. doi: 10.1016/j.semcancer.2011.10.001

9. Shalaby T, Fiaschetti G, Nagasawa K, Shin-ya K, Baumgartner M et al. G-quadruplexes as potential therapeutic targets for embryonal tumors. Molecules 2013; 18 (10): 12500-12537. doi: 10.3390/molecules181012500

10. Blackburn EH. Telomeres. Trends in Biochemical Sciences 1991;16(10):378-381.doi:10.1016/0968-0004(91)90155-O

11. Blasco MA. Telomerase beyond telomeres. Nature Reviews Cancer 2002; 2 (8): 627-633. doi:10.1038/nrc862

12. Luu KN, Phan AT, Kuryavyi V, Lacroix L, Patel DJ. Structure of the human telomere in K+ solution: an intramolecular (3+ 1) G-quadruplex scaffold. Journal of the American Chemical Society 2006; 128 (30): 9963-9970. doi: 10.1021/ja062791w

13. Dai JX, Punchihewa C, Ambrus A, Chen D, Jones RA et al. Structure of the intramolecular human telomeric G-quadruplex in potassium solution: a novel adenine triple formation. Nucleic Acids Research 2007; 35 (7): 2440-2450. doi: 10.1093/nar/gkm009

14. De Cian A, Cristofari G, Reichenbach P, De Lemos E, Monchaud D et al. Reevaluation of telomerase inhibition by quadruplex ligands and their mechanisms of action. Proceedings of the National Academy of Sciences 2007; 104 (44): 17347-17352. doi: 10.1073/pnas.0707365104

15. Yang D, Okamoto K. Structural insights into G-quadruplexes: towards new anticancer drugs. Future Medicinal Chemistry 2010; 2 (4): 619-646. doi: 10.4155/fmc.09.172

16. Balasubramanian S, Hurley LH, Neidle S. Targeting G-quadruplexes in gene promoters: a novel anticancer strategy? Nature Reviews Drug Discovery 2011; 10 (4): 261-275. doi: 10.1038/nrd3428

17. Miller KM, Rodriguez R. G-quadruplexes: selective DNA targeting for cancer therapeutics? Expert Review of Clinical Pharmacology 2011; 4 (2): 139-142. doi: 10.1586/ecp.11.4

18. Xu H, Di Antonio M, McKinney S, Mathew V, Ho B et al. CX-5461 is a DNA G-quadruplex stabilizer with selective lethality in BRCA1/2 deficient tumors. Nature Communications 2017; 8: 14432-14450. doi: 10.1038/ncomms14432

19. Çetinkol ÖP, Engelhart AE, Nanjunda RK, Wilson WD, Hud NV. Submicromolar, selective G-quadruplex ligands from one pot: thermodynamic and structural studies of human telomeric DNA binding by azacyanines. ChemBioChem 2008; 9 (12): 1889-1892. doi: 10.1002/cbic.200800234

20. Velik J, Baliharova V, Fink-Gremmels J, Bull S, Lamka J et al. Benzimidazole drugs and modulation of biotransformation enzymes. Research in Veterinary Science 2004; 79: 95-108. doi: 10.1016/j.rvsc.2003.08.005

21. Khokra SL, Choudhary D. Benzimidazole an important scaffold in drug discovery. Asian Journal of Biochemical and Pharmaceutical Research 2011; 3 (1): 476-486.

22. Hernández-Luis F, Hernández-Campos A, Castillo R, Navarrete-Vázquez G, Soria-Arteche O et al. Synthesis and biological activity of 2-(trifluoromethyl)-1H-benzimidazole derivatives against some protozoa and *Trichinella spiralis*. European Journal of Medicinal Chemistry 2010; 45 (7): 3135-3141. doi: 10.1016/j.ejmech.2010.03.050

23. Tantawy A, Barghash A, Badr S, Gomaa R. Synthesis of new heterocyclic compounds containing benzimidazole moiety as inhibitors of breast cancer cell growth. Heterocyclic Communications 2013; 19 (12): 125-131. doi: 10.1515/hc-2013-0013
24. Mostafa AS, Gomaa RM, Elmorsy MA. Design and synthesis of 2-phenyl benzimidazole derivatives as VEGFR-2 inhibitors with anti-breast cancer activity. Chemical Biology & Drug Design 2019; 93: 454-463. doi: 10.1111/cbdd.13433
25. Maji B, Kumar K, Kaulage M, Muniyappa K, Bhattacharya S. Design and synthesis of new benzimidazole-carbazole conjugates for the stabilization of human telomeric DNA, telomerase inhibition, and their selective action on cancer cells. Journal of Medicinal Chemistry 2014; 57: 6973-6988. doi: 10.1021/jm500427n
26. Shimomura I, Yokoi A, Kohama I, Kumazaki M, Tada Y et al. Drug library screen reveals benzimidazole derivatives as selective cytotoxic agents for KRAS-mutant lung cancer. Cancer Letters 2019; 451: 11-22. doi: 10.1016/j.canlet.2019.03.002
27. Sur S, Tiwari V, Sinha D, Kamran MZ, Dubey KD et al. Naphthalenediimide-linked bisbenzimidazole derivatives as telomeric G-quadruplex-stabilizing ligands with improved anticancer activity. Omega 2017; 2: 966-980. doi: 10.1021/acsomega.6b00523
28. Maji B, Kumar K, Muniyappa K, Bhattacharya S. New dimeric carbazole-benzimidazole mixed ligands for the stabilization of human telomeric G-quadruplex DNA and as telomerase inhibitors. A remarkable influence of the spacer. Organic & Biomolecular Chemistry 2015; 13: 8335-8348. doi: 10.1039/c5ob00675a
29. Kaulage MH, Maji B, Pasadi S, Ali A, Bhattacharya S et al. Targeting G-quadruplex DNA structures in the telomere and oncogene promoter regions by benzimidazole-carbazole ligands. European Journal of Medicinal Chemistry 2018; 148: 178-194. doi: 10.1016/j.ejmech.2018.01.091
30. Yadav K, Meka PNR, Sadhu S, Guggilapu SD, Kovvuri J et al. Telomerase inhibition and human telomeric G-quadruplex DNA stabilization by a β-carboline-benzimidazole derivative at low concentrations. Biochemistry 2017; 56: 4392-4404. doi: 10.1021/acs.biochem.7b00008
31. Pradeep TP, Barthwal R. A 4:1 stoichiometric binding and stabilization of mitoxantrone-parallel stranded G-quadruplex complex established by spectroscopy techniques. Journal of Photochemistry & Photobiology, B: Biology 2016; 162: 106-114. doi: 10.1016/j.jphotobiol.2016.06.019
32. Tariq Z, Barthwal R. Binding of anticancer drug daunomycin to parallel G-quadruplex DNA [d-(TTGGGT)]$_4$ leads to thermal stabilization: a multispectroscopic investigation. International Journal of Biological Macromolecules 2018; 120: 1965-1974. doi: 10.1016/j.ijbiomac.2018.09.154.
33. Das RN, Chevret E, Desplat V, Rubio S, Mergny JL et al. Design, synthesis and biological evaluation of new substituted diquinolinyl-pyridine ligands as anticancer drug agents by targeting G-quadruplex. Molecules 2017; 23 (1): 81. doi: 10.3390/molecules23010081
34. Maiti S, Saha P, Das T, Bessi I, Schwalbe H et al. Human telomeric G-quadruplex selective fluoro-isoquinolines induce apoptosis in cancer cells. Bioconjugate Chemistry 2018; 29: 1141-1154. doi: 10.1021/acs.bioconjchem.7b00781
35. Kumar P, Barthwal R. Structural and biophysical insight into dual site binding of the protoberberine alkoloid palmatine to parallel G-quadruplex DNA using NMR, fluorescence and circular dichroism spectroscopy. Biochimie 2018; 147: 153-169. doi: 10.1016/j.biochi.2018.02.002
36. Jha NS, Mishra S, Mamidi AS, Mishra A, Jha SK et al. Targeting human telomeric G-quadruplex DNA with curcumin and its synthesized analogues under molecular crowding conditions. RSC Advances 2016; 6: 7474-7487. doi: 10.1039/c5ra17390f
37. Tutuncu S, Guloglu S, Kucukakdag A, Çetinkol OP. Selective high binding affinity of azacyanines to polyd(A).polyd (T).polyd(T) triplex: the effect of chain length and branching on stabilization, selectivity and affinity. ChemistrySelect 2018; 3 (45): 12878-12887. doi: 10/1002/slct.201802802

38. Bloomfield VA, Crothers DM, Tinoco I. Nucleic Acids: Structures, Properties, and Functions. Sausalito, CA, USA: University Science Books, 2000.

39. Stulz E, Clever GH. DNA in Supramolecular Chemistry and Nanotechnology. Chichester, United Kingdom: Wiley & Sons Ltd, 2015.

40. Wei C, Jia G, Yuan J, Feng Z, Li CA. Spectroscopic study on the interactions of porphyrin with G-quadruplex DNAs. Biochemistry 2006; 45 (21): 6681-6691. doi:10.1021/bi052356z

41. Horowitz ED, Hud NV. Ethidium and proflavine binding to a 2',5'-linked RNA duplex. Journal of the American Chemical Society 2006; 128 (48): 15380-15381. doi: 10.1021/ja065339I

42. Qu X, Chaires JB. Analysis of drug-DNA binding data. Methods in Enzymology 2000; 321: 353-369. doi: 10.1016/S0076-6879(00)21202-0

43. Haddadin MJ, Kurth MJ, Olmstead MM. One-step synthesis of new heterocyclic azacyanines. Tetrahedron Letters 2000; 41 (30): 5613-5616. doi: 10.1016/S0040-4039(00)00908-4

44. Huang KS, Haddadin MJ, Olmstead MM, Kurth MJ. Synthesis and reactions of some heterocyclic azacyanines. The Journal of Organic Chemistry 2001; 66 (4): 1310-1315. doi: 10.1021/jo001484k